Proceedings of IDETC'05
2005 ASME International Design Engineering Technical Conferences and Computers and Information in Engineering Conference
Long Beach, California, USA, September 24-28, 2005

DETC2005-85618

A HIERARCHICAL APPROACH FOR DESIGN AND ASSEMBLY OF MECHANISMS

Bharath Mukundakrishnan *
GRASP†
University of Pennsylvania
Philadelphia, Pennsylvania 19104
Email: bharathm@grasp.upenn.edu

Vijay Kumar
GRASP
University of Pennsylvania
Philadelphia, Pennsylvania 19104
Email: kumar@grasp.upenn.edu

Peng Song
Mechanical and Aerospace Engineering
Rutgers University
New Brunswick, New Jersey 08854
Email: pengsong@jove.rutgers.edu

J.C. Trinkle
Computer Science
Rensselaer Polytechnic Institute
Troy, NY 12180
Email: trink@cs.rpi.edu

Jong-Shi Pang
Decision Sciences and Engineering Systems
Rensselaer Polytechnic Institute
Troy, NY 12180
Email: pangj@rpi.edu

ABSTRACT

We introduce a hierarchical approach for the analysis and design of systems with multiple frictional contacts, with a focus on applications to the design of part feeding and assembly processes. The simplest model in the hierarchy is the geometric model described by a set of non-penetration constraints that depends only on the geometry of the design. The model with the highest fidelity is one that incorporates rigid body dynamics, joint constraints, and frictional contacts. Our approach is based on a scheme that first uses Rapidly-exploring Random Trees (RRTs) to explore and prune the feasible set of design parameters. The next step is to redesign the system iteratively with the pruned parameter set using a model with higher fidelity. This process is repeated with improved models, until an optimal design is obtained with the model of desired fidelity. We illustrate the models, the design process, and the feasibility of this hierarchical approach by applying it to the design of a simple part feeder.

*Address all correspondence to this author.
†The General Robotics, Automation, Sensing and Perception Laboratory

1 Introduction

There are many manufacturing processes in which nominally rigid bodies undergo frictional contacts, possibly involving impacts. Examples of such processes include part-feeding, assembly, fixturing, material handling, and disassembly. In order to understand the complexity of such processes it is useful to consider the part orienting device shown in Fig. 1. A cup-shaped part enters chute "A" in one of two nominal orientations, which we will call "open end up" (on the left) and "open end down" (on the right). The objective of this mechanism is to cause the part to exit chute "C" in the "open end up" configuration regardless of the orientation when entering chute "A". The part is subject to multiple intermittent frictional contacts with the walls of the chutes and the pin "B". It undergoes frictional impacts before either going down the chute or getting stuck inside the device. There are many factors that affect this feeding process, including the geometry, physical properties of the device and the part's initial condition.

Typically, the preliminary design of such systems is based on intuition, and the detailed design is refined empirically via prototyping. If the prototype does not function properly, as is usually the case in the first several trials, there is no systematic approach

to redesign because the design constraints of such systems are dominated by unilateral constraints and repeated transitions between contact states. Also, the dynamics of part feeding and assembly processes are notoriously difficult to predict because the dynamic models for systems with unilateral constraints are vastly inadequate, and in some cases, do not exist. This is true even for the case of deterministic models. In the past, geometric and quasi-static approaches have been developed for planning manipulation [1–4], assembly [5, 6], part feeding [7], fixturing [8, 9], and grasping tasks [10]. The dynamics of systems with multiple frictional contacts and impacts have been analyzed in [11–14]. However, there is no systematic approach to planning/design for systems with dynamics [15], especially when dynamics are non-smooth.

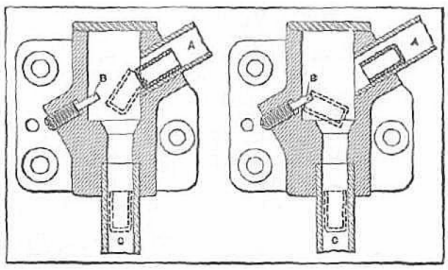

Figure 1. THE EXIT ORIENTATION OF THE CUP-SHAPED PART MUST BE WITH THE OPEN END UP, REGARDLESS OF THE ENTERING ORIENTATION [16].

A schematic of the design problem is given in Fig. 2. Let $X \subset \mathcal{R}^{n_x}$ be the state space for the dynamic system and $P \subset \mathcal{R}^{n_p}$ be the set of parameters (constants) that characterize the geometry (e.g., shape), the inertial properties (e.g., mass) and material properties (e.g., stiffness). The Cartesian product of these sets will be denoted by $\mathcal{Z}$. The set of all system parameters ($\mathcal{Z}_0$) for such systems consist of initial conditions and other parameters that may characterize the system. i.e. $\mathcal{Z}_0 = \{X_0 \times P\}$, where X_0 is the set of initial conditions and P is the set of design parameters, the dimensions of which are determined by the problem at hand. We are interested in two disjoint sets of points in $\mathcal{Z}$ that characterize significant states of the system. The first set $\mathcal{Z}_G$ is the set of all goal states and parameter values. The "unsafe" set $\mathcal{Z}_U$ is the set of points that the system must avoid for the successful completion of the task. The feasible set $\mathcal{Z}_F$ consists of points from which appropriate inputs can steer the system to the goal set $\mathcal{Z}_G$. The set $\mathcal{Z}_A$, are those for which no trajectory passing through them can be steered to $\mathcal{Z}_G$.

It is unreasonable to expect to obtain an exact description of $\mathcal{Z}_A$, $\mathcal{Z}_F$, and $\mathcal{Z}_U$. However, even *partial knowledge* of these sets (inset with light shading in the figure) can significantly reduce the computational cost of planning and improve the robustness of these plans when executing manipulation tasks. These observations lead to the idea of using a hierarchical approach to generate designs such that the optimal design with a desired fidelity can be obtained through refining the parameter set by using models at different levels of hierarchy with different levels of fidelity.

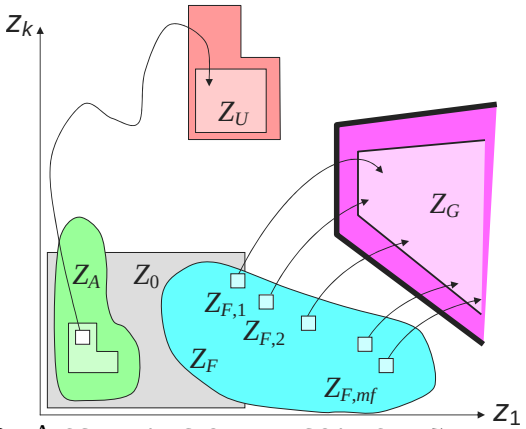

Figure 2. A SCHEMATIC OF THE GOAL SET $\mathcal{Z}_G$, THE UNDESIRABLE OR UNSAFE SET $\mathcal{Z}_U$, THE SET $\mathcal{Z}_A$ CONSISTING OF POINTS THAT ARE GUARANTEED (REGARDLESS OF THE APPLIED INPUTS) TO LEAD TO THE UNSAFE SET, AND THE FEASIBLE SET $\mathcal{Z}_F$ CONSISTING OF POINTS FROM WHICH APPROPRIATE INPUTS CAN STEER THE SYSTEM TO THE GOAL SET. THE DESIGN GOAL IS TO IDENTIFY THE SET $\mathcal{Z}_0$.

In the next section, we present a family of time-stepping models ranging from a simple geometric model, to the more complete dynamic model for systems with intermittent contacts. These model are built on the recent results in the analysis and simulation of non-smooth dynamical systems by the authors of this paper [14, 17–20] and others [21, 22]. A twelve-parameter design problem of the part-feeding device in Fig. 1 is given in Section 3. Section 3 also describes the geometric and kinematic feasibility analysis using the RRT algorithm. Section 4 illustrates results obtained with the dynamic model. This is followed by a discussion in Section 5.

2 Time-Stepping Models

The dynamic equation of motion for a multibody system with contact interactions can be written in the form

$$M(q)\dot{\nu} = u(t,q,\nu) + W_{\mathrm{n}}(q)\lambda_{\mathrm{n}} + W_{\mathrm{t}}(q)\lambda_{\mathrm{t}} + W_{\mathrm{o}}(q)\lambda_{\mathrm{o}}, \qquad (1)$$

where q is the n_q-dimensional vector of generalized coordinates, ν is the n_ν-dimensional vector of generalized velocities, $M(q)$ is the $n_\nu \times n_\nu$ symmetric positive definite inertia matrix and $u(t,q,\nu) \in U \subset \mathcal{R}^{n_\nu}$ is the external force vector (excluding contact forces). $\lambda_{\mathrm{n,t,o}}$ are the n_c-dimensional concatenations of the

contact forces in the normal direction (labelled n) and the two tangential directions (labelled t and o), where n_c is the number of contacts. $W_{\mathrm{n,t,o}}(q)$ are the $n_\nu \times n_c$ Jacobian matrices corresponding to the contact forces. The kinematic equations relate the generalized velocity ν to the time-derivative of the system configuration $\dot{q} \equiv dq/dt$ via a $n_q \times n_\nu$ parameterization matrix $G(q)$:

$$\dot{q} = G(q)\nu. \tag{2}$$

To complete the formulation of the model, we need to include the contact conditions. In the normal direction, the contact condition of the system is governed by

$$0 \le \lambda_{in} \perp \psi_{in} \ge 0, \quad i = 1 \ldots n_c, \tag{3}$$

where $\perp$ denotes complementarity condition and ψ_{in} is the normal separation between contacting objects at the ith contact.

In the tangential direction, the contact conditions are formulated by requiring that friction forces maximize the energy dissipation rate over the sets of admissible contact forces computed based on the friction model. For Coulomb's quadratic cone with friction coefficient μ_i, the maximum dissipation principle at the ith ($i = 1 \ldots n_c$) contact can be written as

$$(\lambda_{it}, \lambda_{io}) = \operatorname{argmin}\{(s_{it}\lambda_{it} + s_{io}\lambda_{io} : (\lambda_{it}, \lambda_{io}) \in \mathcal{F}(\mu_i\lambda_{in})\}$$

where

$$\mathcal{F}(\mu_i\lambda_{in}) \equiv \left\{(\lambda_{it}, \lambda_{io}) : \sqrt{\lambda_{it}^2 + \lambda_{io}^2} \le \mu_i\lambda_{in}\right\}, \tag{4}$$

and s_{it} and s_{io} represent the components of the slip velocity at the ith contact.

The quadratic cone can be linearized using the following polyhedral approximation, at any $i = 1 \ldots n_c$:

$$\widehat{\mathcal{F}}(\mu_i\lambda_{in}) \equiv \{W_{if}\lambda_{if} : \|\lambda_{if}\|_1 \le \mu_i\lambda_{in}, \lambda_{if} \ge 0\} \tag{5}$$

where W_{if} is a $2 \times n_f$ matrix whose columns are coplanar vectors that positively space the contact tangent plane (the t-o plane), λ_{if} is a vector of friction force magnitudes corresponding to the columns of W_{if}, and n_f is the number of edges of the polyhedral approximation of the friction cone. Note that the jth component of λ_{if} is the magnitude of the friction force along the direction defined by column j of W_{if}. The following complementarity conditions can be derived from the the maximum dissipation principle problem as:

$$\begin{array}{l} 0 \le s_i e_i + W_{if}^T \nu \perp \lambda_{if} \ge 0 \\ 0 \le \mu_i\lambda_{in} - e_i^T\lambda_{if} \perp s_i \ge 0 \end{array}, \tag{6}$$

where s_i is a slack variable that approximates the magnitude of the slip velocity at contact i, and e_i is an n_f-vector of ones.

Together, Eqns.(1), (2), (3), and (4) or (6) constitute the equations of motion which have four components: the dynamics of the mechanical system, the kinematic map, the normal contact conditions, and the friction law.

We consider a time discretization of the differential equations (1) and (2) for $t \in (0, T]$. Fix a positive integer N and let $h \equiv T/N$. Partition the interval $[0, T]$ into N subintervals $[t_\ell, t_{\ell+1}]$, where $t_\ell \equiv \ell h$, for $\ell = 0, 1, \ldots, N$. Write

$$q^\ell \equiv q(t_\ell), \quad \nu^\ell \equiv \nu(t_\ell), \quad \text{and} \quad \lambda_{\mathrm{n,t,o}}^\ell \equiv \lambda_{\mathrm{n,t,o}}(t_\ell).$$

The time derivatives $\dot{\nu}$ and $\dot{q}$ are replaced by the backward Euler approximations: for all $\ell = 0, \ldots, N-1$,

$$\dot{\nu}(t_{\ell+1}) \approx \frac{\nu^{\ell+1} - \nu^\ell}{h} \quad \text{and} \quad \dot{q}(t_{\ell+1}) \approx \frac{q^{\ell+1} - q^\ell}{h}.$$

The various time-stepping schemes differ in how $M(q)$ and the right-hand sides in Eqns.(1) and (2) are approximated.

2.1 Rigid Body Dynamic Model

Stewart and Trinkle [23] developed a semi-implicit time-stepping method that originally formulated each time step as a mixed linear complementarity problem (mixed LCP) in terms of the unknown generalized velocity $\nu^{\ell+1}$, the normal and frictional impulses $(p_{\mathrm{n}}^{\ell+1}, p_{\mathrm{f}}^{\ell+1})$ (defined as: $p_{\mathrm{n}}^{\ell+1} = h\lambda_{\mathrm{n}}^{\ell+1}$, $p_{\mathrm{f}}^{\ell+1} = h\lambda_{\mathrm{f}}^{\ell+1}$), and the slack variable $s^{\ell+1}$. However, the generalized velocity can be eliminated by using the equation of motion, thereby allowing reformulation of the time-stepping method as a standard LCP(B, b) written as follows:

$$\begin{array}{r} \nu^{\ell+1} = B^\ell z^{\ell+1} + b^\ell \\ 0 \le \nu^{\ell+1} \perp z^{\ell+1} \ge 0 \end{array} \tag{7}$$

with B^ℓ, b^ℓ, and $z^{\ell+1}$ given as follows:

$$B^\ell = \begin{pmatrix} W_{\mathrm{n}}^T M^{-1} W_{\mathrm{n}} & W_{\mathrm{n}}^T M^{-1} W_{\mathrm{f}} & 0 \\ W_{\mathrm{f}}^T M^{-1} W_{\mathrm{n}} & W_{\mathrm{f}}^T M^{-1} W_{\mathrm{f}} & E \\ U & -E^T & 0 \end{pmatrix}$$

$$b^\ell = \begin{pmatrix} W_{\mathrm{n}}^T(\nu + M^{-1}uh) + \psi_{\mathrm{n}}(q^\ell)/h \\ W_{\mathrm{f}}^T(\nu + M^{-1}uh) \\ 0 \end{pmatrix}, \; z^{\ell+1} = \begin{pmatrix} p_{\mathrm{n}}^{\ell+1} \\ p_{\mathrm{f}}^{\ell+1} \\ s^{\ell+1} \end{pmatrix},$$

where E is a block diagonal matrix, with each diagonal block equal to a column vector length n_f with all elements equal to

one. U is a diagonal matrix of size n_c with element (i,i) equal to μ_i.

Several points are worth noting. First, the term $\psi_n(q^\ell)/h$ provides constraint stabilization with $\psi_n(q^\ell)$ being the vector of the normal separations between each pair of bodies in or about to be in contact. When it is negative (implying interpenetration of bodies), it acts to generate a bias impulse that increases the normal component of the relative velocity at a contact large enough to eliminate the penetration at the end of the next time step. Second, there is no restitution law built into this formulation. To include bouncing effects, one must stop the Stewart-Trinkle method at the time of each collision and apply an impact model. Third, in order to obtain the timestep subproblem as a linear rather than nonlinear complementarity problem, the quadratic friction cone and non-interpenetration constraints were linearized. Fourth, also critical to obtaining an LCP, the quantities (such as M and W_n) are explicit functions of the state, i.e., they depend only on current or past states.

2.2 Kinematic model

Our kinematic model is a first order approximation of the dynamic model. Instead of treating forces as inputs, we want to think of input velocities. These control inputs u are constrained to lie in a bounded set U as in the case of the dynamic model. However, the set U now is the set of available velocities. At time instant ℓ, the set of available velocities is denoted by $U^{\ell+1}$. Note that while this model captures first order kinematic constraints and geometric constraints, it is not guaranteed to produce trajectories that are consistent with rigid body dynamics. Our model is as follows.

$$\begin{aligned} q^{\ell+1} - q^\ell &= h\,G(q^\ell)\nu^{\ell+1} \\ \nu^{\ell+1} &= \bar{W}(q^\ell)u^{l+1} \\ \psi_n(q^{\ell+1}) &\geq 0 \end{aligned} \tag{8}$$

where $\bar{W}(q^\ell)$ is the Jacobian that incorporates kinematic constraints.

2.3 Geometric model

Our geometric model is a zeroth order approximation of the dynamic model. Instead of treating forces or velocities as inputs, we simply consider increments in position. The contribution inputs u are now position (and orientation) increments that are constrained to lie in a bounded set U. While the predicted motions are guaranteed to conform to geometric constraints, the trajectories may not satisfy kinematic or dynamic constraints. The geometric constraints are simply described by a set of non-penetration constraints represented by semi-algebraic sets constructed with distance functions. However when simulating a system over a small time step starting from a geometrically generic configuration, the non-penetration conditions can usually be expressed as a conjunction of non-negativity constraints on the relevant distance function. The model is as follows.

$$\begin{aligned} q^{\ell+1} - q^\ell &= h\,G(q^\ell)u^{\ell+1} \\ u^{\ell+1} &\in U^{\ell+1} \\ \psi_n(q^{\ell+1}) &\geq 0 \end{aligned} \tag{9}$$

3 Design of the Part Feeding System

For the part feeding system described in Section 1, given a rectangular peg with fixed dimensions, mass, and moment of inertia, the goal is to determine the optimal design of the feeder such that a peg entering the feeder with different orientations (as shown in Fig. 10 and Fig. 11) always exits in the orientation with the center of gravity down. A secondary objective is to have the peg pass through the device as quickly as possible. The mechanism for peg insertion problem with the design parameters is described in Fig. 3.

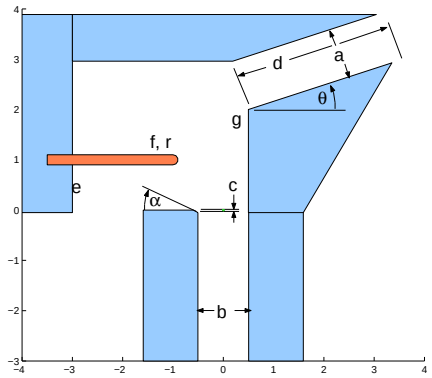

Figure 3. REORIENTING DEVICE WITH DESIGN VARIABLES.

The parameter space (design space P) is twelve-dimensional (See Table 1). In practice, given the dimension of such systems, it is difficult to guarantee the convergence to the design optimization problem with the dynamic model. The key idea here is instead of computing the the dynamically feasible sets of P directly, we first determine a feasible subset using the geometric model in Eqn.(9). This is then followed by further analysis using the kinematic model in Eqn.(8) and finally with the dynamic model in Eqn.(7). At each step, the size of the feasible set is reduced thus decreasing the search space for successive refinements.

Instead of working with the continuous design space, we sample the design space P to generate a discrete set of design choices. Thus, we start with a discrete set of points ($P_s \subset P \in$

Table 1. DESIGN SPACE (P) PARAMETERS AND THEIR DEFINITIONS.

Parameter	Definition
a	width of input chute
b	width of output chute
c	depth of chamfer
d	length of input chute
e	horizontal location of left cavity wall
f	position of center of tip of protuberance
g	position of lower left corner of chute
r	radius of protuberance
θ	angle of input chute
α	angle of chamfer

$\Re^{12}$) sampled uniformly [1] using a Halton sequence [24]. Each point in P_s corresponds to a polygonal model of the part feeder which can be automatically generated. This polygonal description is triangulated using *Triangle* [25]. The *PQP* collision detection scheme [26] is used for collision detection to enforce non-penetration constraints.

Geometric feasibility of the given set of design parameters can be systematically determined by the use of RRT algorithm. The RRT algorithm [27] is designed for efficient search of state space to obtain a feasible set of states subject to problem constraints (e.g., geometric, kinematic or dynamic constraints). The configuration x of the peg is defined by its position and orientation. The RRT tree $\mathcal{T}$ is initialized by a single initial configuration x_{ini} drawn at random from the space of configurations $\mathcal{C}$ (C-space). Then a new candidate configuration $x_{rand} \in \mathcal{C}$ is chosen. The configuration $x_{near} \in \mathcal{T}$, closest to x_{rand}, is determined using the metric $\rho_1(x_{rand}, x_{near})$. New feasible configurations (x_{new}) that minimize the metric $\rho_2(x_{rand}, x_{new})$ are obtained by using the model in Eqn. 9. These configurations are added to the RRT tree $\mathcal{T}$. This process is iterated until $x_{desired}$ is obtained or a maximum number of iterations is attained. This RRT algorithm is iterated over P to achieve a geometrically feasible subset of design parameters. This extended RRT algorithm is given in Algorithm (1).

The metric functions ρ_1 and ρ_2 that determine the nodes of the explored RRT tree are simply Euclidean metrices with additional weights to reconcile the differences in units and scales of the different elements in x. A more elaborate discussion on the choice of metrics and the algorithm can be found in [28].

A sample RRT for a given set of geometrically feasible parameters is shown in Fig. 4. The RRT finds geometrically feasible paths (thin line) for the peg through the device for the given design parameters. The thick line shows the path of the center of mass for a successful feasible path from the start position and orientation to the goal.

Algorithm 1 GENERATE PEGRRT: $\mathcal{T}$

```
Input parameter space P, P ∈ ℜ^12
Uniformly sample P and determine P_s ⊂ P ∈ ℜ^12
for P_i ∈ P_s do
  Map P_i to geometry of part feeder S ∈ ℜ^2
  Read Input: max_iterations, steps, time, C, U, x_ini, x_desired
  Initialize RRT: T.addNode(x_ini)
  while max_iterations do
    Generate random node: x_rand ∈ C
    x_near ← min_{x_j ∈ T} ρ1(x_rand, x_j)
    h = (time / steps)
    for u ∈ U do
      for steps do
        x_curr = x_old + u.h
        if Collision(S, x_curr) then
          break
        end if
        x_old = x_curr
      end for
      x_new = min_{u∈U} {x_new, ρ2(x_rand, x_curr)}
    end for
    T.addNode(x_new)
    T.addEdge((u ∈ U), x_near → x_new)
    if x_new ≈ x_desired then
      break
    end if
  end while
  Store parameter set P_i and T
end for
```

One can also use this algorithm to explore trajectories over a range of parametric values. For example, by sampling uniformly over the set of all possible input chute angles θ, we can find those chute angles that lead to successful trajectories. In Fig. 5 two samples of geometric feasible paths are shown for $\theta = 0.235$ and $\theta = 0.529$.

We can also use this approach to uniformly sample the entire twelve-dimensional parameter space in the range specified in Table 2. Results of two successful trials are given in Fig. 6. This process allows us to eliminate infeasible design parameters that result in unsuccessful trajectories thus resulting in a smaller search space for the design optimization with dynamic models. See Fig. 7 for designs corresponding to such infeasible design parameters.

[1] The Halton sequence is a quasi-random sequence of points that is known to minimize the discrepancy measure [24].

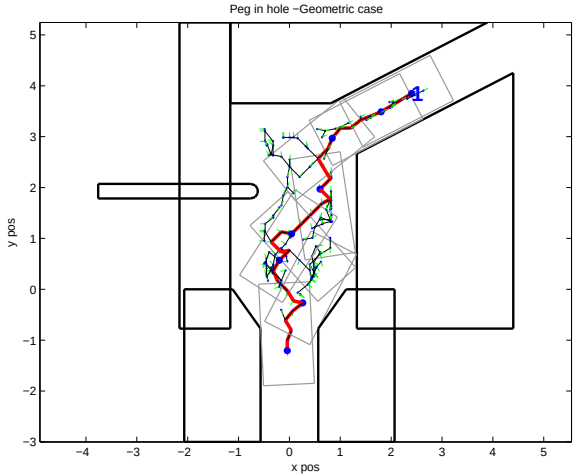

Figure 4. A SAMPLE RRT WHICH INCLUDES A GEOMETRICALLY FEASIBLE *successful* PATH FOR THE PART (THICK LINE) WITH BRANCHES DENOTING OTHER GEOMETRICALLY FEASIBLE TRAJECTORIES (THIN LINE). THE PARAMETERS ARE: $(a = 1.113, b = 1.134, c = 0.7727, d = 3.462, e = -1.161, f = (-0.616, 1.929), g = (1.325, 2.666), r = 0.144, \theta = 0.4764, \alpha = 0.9526)$.

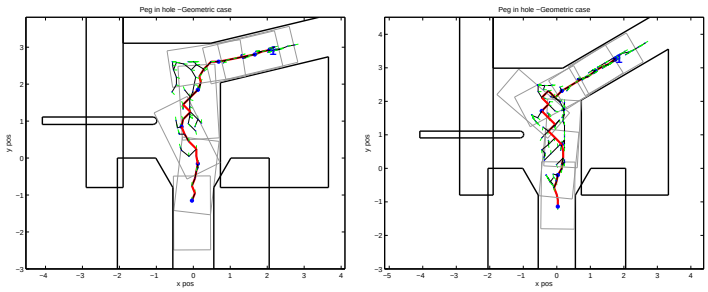

Figure 5. THE RRT RESULT SHOWS THAT BOTH CHUTE ANGLES $\theta = 0.235$ AND $\theta = 0.529$ LEAD TO SUCCESSFUL GEOMETRICALLY FEASIBLE SOLUTIONS FOR THE PARAMETER VALUES $(a = 1.1, b = 1.1086, c = 0.798, d = 3.008, e = -1.9, f = (-0.985, 1.01), g = (0.733, 2.039), r = 0.101, \alpha = 1.047)$.

Table 2. PARAMETER SET P FOR PART FEEDER DESIGN.

Parameter	Range	Parameter	Range
a	[1.1,1.2]	f	x = [-1.0,-0.6]× y = [0.5,2.5]
b	[1.1,1.3]	g	x = [0.2,2.0]× y = [1.5,3.0]
c	[0.75,0.8]	r	[0.1,0.3]
d	[2.5,5]	θ	[0.3,0.9]
e	[-1.0,-2.0]	α	[0.9,1.1]

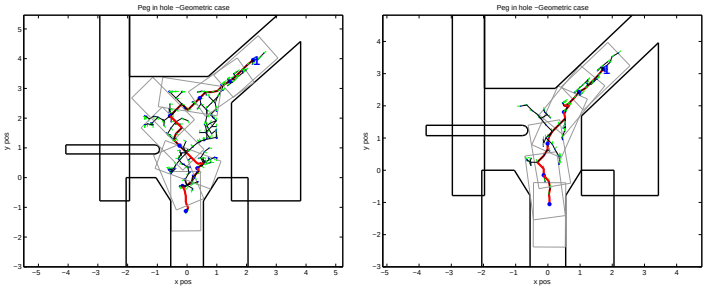

Figure 6. THE RRT ALGORITHM SUCCESSFULLY FINDS A GEOMETRICALLY FEASIBLE PATH. THE PARAMETER VALUES FOR THE LEFT AND RIGHT FIGURES ARE $(a = 1.178, b = 1.1, c = 0.782, d = 3.106, e = -1.935, f = (-0.923, 0.949), g = (1.493, 2.518), r = 0.152, \theta = 0.725, \alpha = 1.005)$ AND $(a = 1.181, b = 1.107, c = 0.787, d = 3.298, e = -1.967, f = (-0.619, 1.234), g = (1.043, 1.685), r = 0.161, \theta = 0.761, \alpha = 1.016)$.

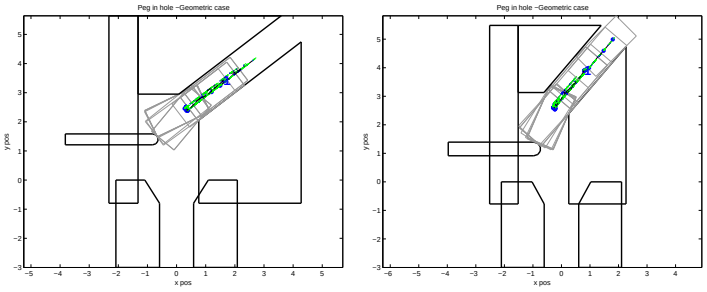

Figure 7. SAMPLE RRTS FOR PARAMETER VALUES FOR WHICH THE ALGORITHM DID NOT RETURN A SUCCESSFUL TRAJECTORY FOR PEG REORIENTATION. THE PARAMETER VALUES FOR THE LEFT AND RIGHT FIGURES ARE $(a = 1.1, b = 1.1, c = 0.75, d = 2.5, e = -1.0, f = (-0.6, 0.5), g = (0.2, 1.5), r = 0.1, \theta = 0.3, \alpha = 0.9)$ AND $(a = 1.127, b = 1.168, c = 0.795, d = 4.423, e = -1.322, f = (-0.632, 1.397), g = (0.762, 2.055), r = 0.186, \theta = 0.65, \alpha = 1.005)$.

The kinematic model (Eqn. 8) enforces the non-penetration constraint by determining impulsive forces during collision based on the impact model described in [29]. The kinematic model is used to further prune the discrete set of geometrically feasible design points in the design space. This smaller subset of geometrically and kinematically feasible design points are used as initial values for further analysis and optimization with the dynamic model. The RRT Algorithm (1) is modified as shown in the Algorithm (2).

Algorithm 2 GENERATE KINEMATIC PEGRRT: $\mathcal{T}$

...
...
if $Collision(S, x_{curr})$ **then**
  Calculate Impulse: $Imp(x_{curr}, u_{curr})$
  Update state velocity: $u_{new} \leftarrow u_{curr} + M^{-1} Imp(x_{curr}, u_{curr})$
end if
...
...

Figure.8 shows two kinematically feasible points starting with geometrically feasible design points in the design space P_s.

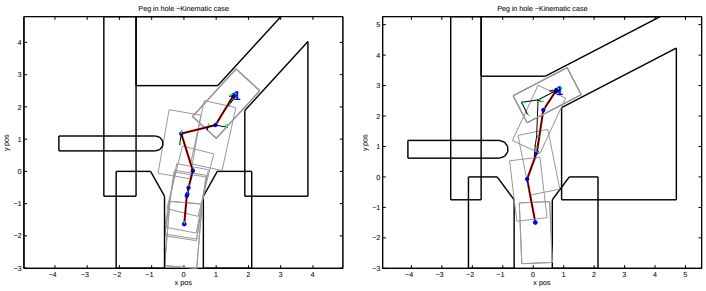

Figure 8. THE RRT ALGORITHM SUCCESSFULLY FINDS A KINEMATICALLY FEASIBLE PATH. THE PARAMETER VALUES FOR THE LEFT AND RIGHT FIGURES ARE $(a = 1.14, b = 1.2, c = 0.769, d = 2.899, e = -1.483, f = (-0.65, 0.87), g = (1.88, 1.88), r = 0.23, \theta = 0.829, \alpha = 1.06)$ AND $(a = 1.159, b = 1.25, c = 0.751, d = 4.245, e = -1.709, f = (-0.824, 0.908), g = (0.931, 2.277), r = 0.291, \theta = 0.478, \alpha = 0.932)$.

It is of course possible that the RRT algorithm may terminate after a prescribed maximum number of iterations even if the design parameters may be geometrically feasible. One can run the algorithm for more iterations and find if a solution indeed exists. But often we are only interested in finding *a* set of feasible solutions rather than all possible solutions. Geometric and kinematic feasibility analysis using the RRT algorithm provides a computationally efficient way to prune the design space, which will enable convergence of the design optimization problem with dynamic models.

4 Dynamic analysis of the part feeding mechanism

Geometrically and kinematically feasible design parameters for the dynamic analysis are chosen from the range of design parameters in Table. 2. The RRT results corresponding to a set of initial design parameters are shown in Fig. 9. The design problem with the dynamic models is expressed as an optimization problem with the design space (P) specified by simple bounds placed on the twelve design variables and the objective function given as follows:

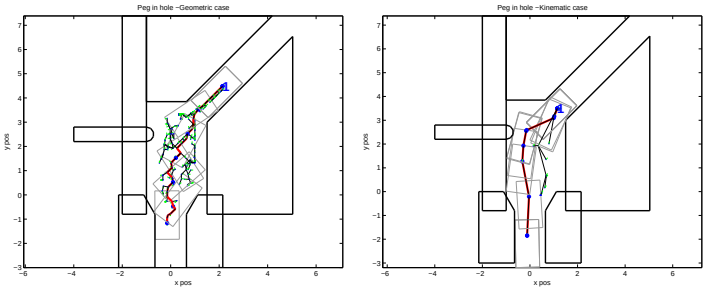

Figure 9. THE RRT GENERATED FOR THE SET OF PARAMETERS $(a = 1.2, b = 1.3, c = 0.8, d = 5, e = -1.0, f = (-0.7, 2.5), g = (1.5, 3), r = 0.3, \theta = 0.7854, \alpha = 1.0472)$ SHOWING A SUCCESSFUL GEOMETRICALLY FEASIBLE TRAJECTORY (LEFT) AND KINEMATICALLY FEASIBLE TRAJECTORY (RIGHT). THIS IS USED AS AN INITIAL GUESS FOR GENERATING A SUCCESSFUL DYNAMICALLY FEASIBLE DESIGN OF PART FEEDER.

$$\mathcal{G} = \sum_{i=1}^{2} w \, ||q_i(T_i) - q_{\text{goal}}|| + T_i \tag{10}$$

where q_{goal} is a target configuration of the peg at some point well within the exit chute, T is the time when the peg either comes to rest or when the y component of its center of gravity moves below that of q_{goal}, w is a weight factor and $i \in \{1, 2\}$ with 1 or 2 indicating that the peg entered the input chute with the heavy end of the peg on top or bottom of the chute. With this objective function, the design problem can be written as

$$P = \min \mathcal{G}(X, T) \quad \text{s.t. } \dot{X} = \mathcal{F}_Q(X, P), \tag{11}$$

where the parameter set P is the set of all the twelve design variables given in Table. 1, the states variable $X \equiv (q, \dot{q})$. The function $\mathcal{F}_Q(X, P)$ is given by Eqn.(7).

The dynamic simulation was carried out in Matlab using the constrained optimization routine, `fmincon`, with the time-stepping dynamic method called twice for each objective function evaluation. Figures 10 and 11 show the result obtained after

approximately 1000 objective function evaluations. The weight factor w in the objective function is set to be 5. Note that the peg falls through the device in the proper orientation regardless of its entering orientation. The optimal design parameters found from dynamic analysis are tabulated in Table. 3.

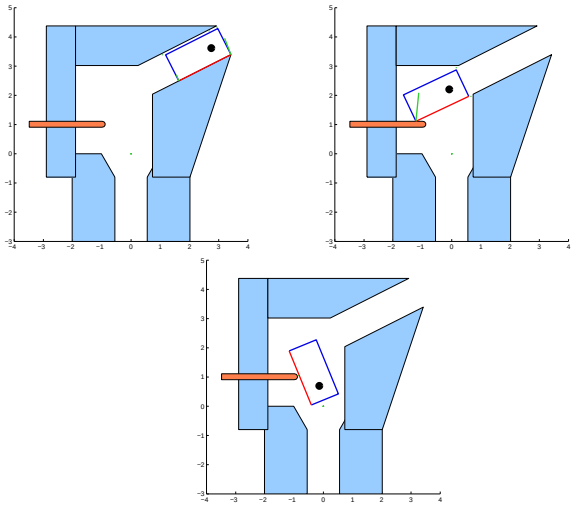

Figure 10. THREE SNAPSHOTS OF A DYNAMICALLY CORRECT TRAJECTORY SHOWING THAT THE PEG IS ABLE TO PASS THROUGH THE DEVICE WITH THE DESIGN PARAMETERS FOUND BY THE OPTIMIZATION ALGORITHM. THE HEAVY END OF THE PEG IS ON TOP IN THE INITIAL CONFIGURATION.

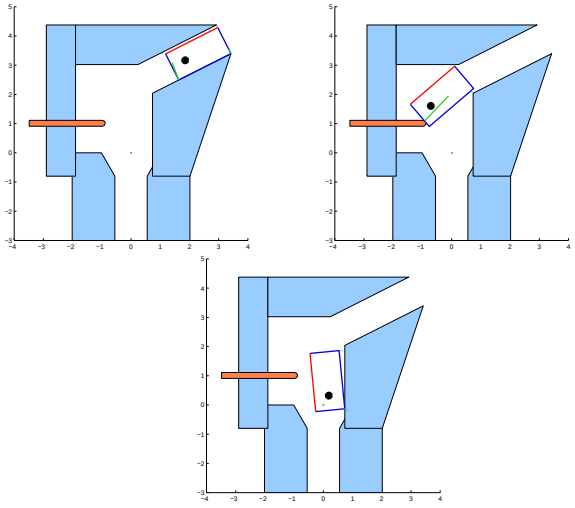

Figure 11. THREE SNAPSHOTS OF A DYNAMICALLY CORRECT TRAJECTORY SHOWING THAT THE PEG IS ABLE TO PASS THROUGH THE DEVICE WITH THE DESIGN PARAMETERS FOUND BY THE OPTIMIZATION ALGORITHM. THE HEAVY END OF THE PEG IS FED THROUGH THE CHUTE FIRST IN THE INITIAL CONFIGURATION.

Table 3. OPTIMAL VALUES OF PARAMETERS WITH DYNAMIC MODEL.

Parameter	Value	Parameter	Value
a	1.1	f	[-0.9849,1.0098]
b	1.1086	g	[0.733,2.0388]
c	0.7979	r	0.101
d	3.0078	θ	0.4673
e	-1.9	α	1.0472

5 Discussion

The ultimate goal of our research is to be able to automatically generate motion plans (inputs) and designs (initial conditions and parameters) for part feeding and assembly operations. The problem of finding the feasible sets of initial conditions and design parameters to plan trajectories for manipulation tasks is similar to *motion planning problem* in robotics where the goal is: given a robot with dynamics and constraints (obstacles), find a path or trajectory (if one exists) from the starting configuration to the goal configuration. Just as complete motion planning is hard to obtain for complex problems, we may not be able to develop complete algorithms, or prove correctness or safety.

In this paper, we present three models that lend themselves to hierarchical design and planning of manipulation tasks. Our approach allows us to boot-strap the design optimization process with a low-resolution model that is used to find geometrically feasible initial plans quickly without difficulties of convergence with limited computational resources. This initial plan is then refined in successive iterations by upgrading to models with higher resolution and fidelity.

ACKNOWLEDGMENT

The RRT model geometries were generated using *Triangle* software developed by Jonathan Richard Shewchuk [25]. Support from NSF grants DMS01-39747, Davinci IIS-0413138 and IIS02-22927 are gratefully acknowledged.

REFERENCES

[1] Akella, S., Huang, W., Lynch, K., and Mason, M., 1996. "Sensorless parts feeding with a one joint robot". In Workshop on the Algorithmic Foundations of Robotics.

[2] Trinkle, J., and Hunter, J. J., 1991. "A framework for planning dexterous manipulation". In Proceedings of the 1991 IEEE International Conference on Robotics and Automation, pp. 1245–1251.

[3] Trinkle, J., and Zeng, D., 1995. "Prediction of the quasistatic planar motion of a contacted rigid body". *IEEE Transactions on Robotics and Automation*, **11**(2), Apr., pp. 229–246.

[4] Zumel, N., and Erdmann, M., 1996. "Nonprehensible two palm manipulation with non-equilbrium transitions between stable states". In Proceedings of the 1996 IEEE International Conference on Robotics and Automation, pp. 3317–3323.

[5] Donald, B. R., and Pai, D. K., 1990. "On the motion of compliantly connected rigid bodies in contact: a system for analyzing designs for assembly". In Proceedings of the 1990 IEEE International Conference on Robotics and Automation, pp. 1756–1762.

[6] Balkcom, D., and Trinkle, J., 2002. "Computing wrench cones for planar rigid body contact tasks". *The International Journal of Robotics Research,* **21**(12), pp. 1053–1066.

[7] Mirtich, B., Zhuang, Y., Goldberg, K., Craig, J., Zanutta, R., Carlisle, B., and Canny, J., 1996. "Estimating pose statistics for robotic part feeders". In Proceedings of the 1996 IEEE International Conference on Robotics and Automation, pp. 1140–1146.

[8] Wolter, J. D., and Trinkle, J., 1994. "Automatic selection of fixture points for frictionless assemblies". In Proceedings of the 1994 IEEE International Conference on Robotics and Automation, Vol. 1, pp. 528–534.

[9] Zhang, T., and Goldberg, K., 2002. "Gripper point contacts for part alignment". *IEEE Transactions on Robotics and Automation,* **18**(6), pp. 902–910.

[10] Cherif, M., and Gupta, K., 1997. "Planning quasi-static motions for re-configuring objects with a multi-fingered robotic hand". In Proceedings of the 1997 IEEE International Conference on Robotics and Automation.

[11] Brogliato, B., 1996. *Nonsmooth Impact Mechanics - Models, Dynamics, and Control*. Springer-Verlag, London. Lecture Notes in Control and Information Sciences.

[12] Song, P., Kraus, P., Kumar, V., and Dupont, P., 2001. "Analysis of rigid–body dynamic models for simulation of systems with frictional contacts". *ASME Journal of Applied Mechanics,* **68**, pp. 118–128.

[13] Stewart, D., 2000. "Rigid-body dynamics with friction and impact". *SIAM Review,* **42**, pp. 3–39.

[14] Trinkle, J., Pang, J.-S., Sudarsky, S., and Lo, G., 1997. "On dynamic multi-rigid-body contact problems with coulomb friction". *Zeitschrift für Angewandte Mathematik und Mechanik,* **77**(4), pp. 267–280.

[15] Lynch, K., 1996. "Nonprehensile manipulation: Mechanics and planning". PhD thesis, School of Computer Science, Carnegie Mellon University, Mar.

[16] Boothroyd, G., and Redford, A. H., 1968. *Mechanized Assembly: Fundamentals of parts feeding, orientation, and mechanized assembly*. McGraw-Hill, London.

[17] Song, P., Pang, J.-S., and Kumar, V., 2004. "A semi-implicit time-stepping model for frictional compliant contact problems". *International Journal for Numerical Methods in Engineering,* **60**, pp. 2231–2261.

[18] Stewart, D., and Trinkle, J., 2000. "An implicit time-stepping scheme for rigid body dynamics with coulomb friction". *Proceedings, IEEE International Conference on Robotics and Automation*, pp. 162–169.

[19] Song, P., Trinkle, J., Kumar, V., and Pang, J.-S., 2004. "Design of part feeding and assembly processes with dynamics". *Proceedings, IEEE International Conference on Robotics and Automation*, May, pp. 39–44.

[20] Trinkle, J., Tzitzouris, J., and Pang, J.-S., 2001. "Dynamic multi-rigid-body systems with concurrent distributed contacts: Theory and examples". *Philosophical Transactions: Mathematical, Physical, and Engineering Sciences,* **359**(1789), Decemeber, pp. 2575 – 2593.

[21] Anitescu, M., and Potra, F., 2002. "Time-stepping schemes for stiff multi-rigid-body dynamics with contact and friction". *International Journal for Numerical Methods in Engineering,* **55**, pp. 753 – 784.

[22] Tzitzouris, J., 2001. "Numerical resolution of frictional multi-rigid-body systems via fully-implicit time-stepping and nonlinear complementarity". PhD thesis, Department of Mathematical Sciences, The Johns Hopkins University, Baltimore, MD.

[23] Stewart, D., and Trinkle, J., 1996. "An implicit time-stepping scheme for rigid-body dynamics with inelastic collisions and coulomb friction". *International Journal of Numerical Methods in Engineering,* **39**, pp. 2673–2691.

[24] Halton, J. H., 1960. "On the efficiency of certain quasi-random sequences of points in evaluating multi-dimensional integrals". *Numer. Math.*(2), pp. 84–90.

[25] Shewchuk, J. R., 1996. "Triangle: Engineering a 2D Quality Mesh Generator and Delaunay Triangulator". In *Applied Computational Geometry: Towards Geometric Engineering,* M. C. Lin and D. Manocha, eds., Vol. 1148 of *Lecture Notes in Computer Science*. Springer-Verlag, May, pp. 203–222. From the First ACM Workshop on Applied Computational Geometry.

[26] PQP: A Proximity Query Package, `http://www.cs.unc.edu/~geom/SSV/`, University of N. Carolina, 1999.

[27] LaValle, S. M., and Kuffner, J. J., 2001. "Randomized kinodynamic planning". *International Journal of Robotics Research,* **20**(5), pp. 378–400.

[28] Kim, J., Esposito, J. M., and Kumar, V., 2005. "An RRT-based algorithm for testing and validating multi-robot controllers". *Robotics: Science and Systems Conference, MIT, Cambridge, MA, U.S.A.* Submitted.

[29] Wang, Y. Mason, M., 1992. "Two-dimensional rigid-body collisions with friction". *ASME Journal of Applied Mechanics,* **59**, pp. 635–641.